Overcoming Limitations of Circuit Synthesis in Microwave Filter Design

Vicente E. Boria*, Pablo Soto*, Santiago Cogollos*

*Grupo de Aplicaciones de las Microondas (GAM),

Instituto de Telecomunicaciones y Aplicaciones Multimedia (iTEAM),

Universidad Politécnica de Valencia,

Camino de Vera s/n, E-46022 Valencia, SPAIN,

Phone: +34 96 3879718, Fax: +34 96 3877309,

E-mail:{vboria, pabsopac, sancobo}@dcom.upv.es

Abstract

Microwave Magazine does not publish abstracts. According to an Editors' suggestion, the main ideas pointed out in the abstract have been included in the Introduction Section of the current manuscript.

Index Terms

Circuit synthesis, design methodology, microwave filters, equivalent circuits, distributed parameter circuits, waveguide filters, low-pass filters, bandpass filters, coaxial filters, dual-mode filters.

I. Introduction

Microwave filters are key building blocks of the front ends present in any modern communication system, such as radio and TV broadcasting, mobile communication services or satellite payloads [1]–[3]. According to the needs of each application, filters are required to have different electrical specifications (i.e., in-band amplitude and group delay behavior, as well as out-of-band transmission features) [4], and are implemented in the most suitable transmission medium (typically using coaxial, planar or waveguide technologies) [5]–[7]. Over the years, the design and development of microwave filters have received considerable attention in the technical literature [8], [9].

Although several significant advances in microwave filter design have been achieved over the last decades, many of the design procedures of RF and microwave filters are still based on Cohn's paper from the late 1950s [10]. This classic procedure consists of the three following steps: first, starting from well-known mathematical models, an equivalent circuit prototype (either based on lumped and/or distributed elements) is synthesized [11]; second, after identifying the prototype elements with real structure parts, initial estimates for the physical dimensions are obtained [12], [13]; and third, a final optimization of the filter dimensions is typically performed [14]–[16]. The success of this design procedure is based on the similarities between the equivalent circuit prototype and the real filter structure. However, with the advent of more stringent requirements for filter responses and their physical realization, there is an increasing number of situations where the equivalent circuit models do not behave precisely as the real structures do, thus providing initial physical dimensions far from the final solution.

An impaired starting point makes the task of the optimizer more difficult and often provides an unsatisfactory final structure. For instance, the real implementation of equivalent circuits typically introduces additional effects (e.g., due to discontinuities between different transmission media), that degrade the response of the synthesized structure [17]. On the other hand, filters with moderate or wide bandwidths, as well as filters based on real elements with different frequency dispersive behavior (inhomogeneous structures), require advanced prototypes with frequency-dependent components [18]–[21]. Additionally, with the aim of improving the design procedure of narrowband filters (e.g. dual-mode filters of satellite payloads or side-coupled coaxial cavity filters), the classic equivalent circuits based on lumped-elements can be enhanced with distributed models which behave more like the physical structure [22]–[25].

In this paper, the limitations of the synthesis methods based on classic equivalent circuits will be identified. Then, enhanced distributed models (including the electromagnetic (EM) behavior of the structure's elements) and synthesis procedures able to overcome such restrictions will be presented. These synthesis

techniques are validated through the design of several filters implemented in coaxial and waveguide technology, where the restrictions of circuit-based synthesis methods can often be observed. For such design purposes, all of the authors' enhanced EM-based distributed models and synthesis procedures have been successfully integrated within the ESA (European Space Agency) software package FEST 3D (Full-Wave Electromagnetic Simulation Tool) [26]. This package is based on advanced modal methods, compiled in [27] and first described in [28]–[33].

As an illustrative example of circuit synthesis limitations, we first deal with conventional low-pass corrugated waveguide filters [4]. The behavior of a synthesis procedure directly based on the classic low-pass distributed prototype is compared with two recently published techniques (see [17] and [34]), where the discontinuities between adjacent waveguides of the real filter structure are considered. The results reveal the advantages of working with equivalent prototypes that are as close as possible to the real structures. Next, we consider the accurate circuit synthesis of in-line inductive waveguide filters with moderate and wide bandwidths, implemented through either homogeneous or inhomogeneous structures. It is well known that such filter responses and configurations cannot be directly recovered from classic synthesis methods based on equivalent circuits composed of constant impedance inverters and equal transmission line resonators [4], [5]. The performance of traditional [11], [19] and recent [21], [35] synthesis techniques including frequency-dependent elements are compared through the design of a moderate bandwidth, a wideband and an inhomogeneous H-plane filter. The synthesis technique based on a flexible prototype able to represent the real structure behavior [36] yields the best results.

Lumped-element prototypes directly derived from the coupling matrix do not always represent the structure topology, even for the narrowband case. As a result, an exact one-to-one correspondence between the structure parts and the prototype elements is not always possible, thus hampering the dimensional synthesis of the component. In Section IV, accurate synthesis procedures for both narrowband in-line coaxial cavity filters and dual-mode filters in circular waveguide are outlined. Such methods rely on distributed models [37], [38] with a good correspondence to the real structure. This allows the development of systematic synthesis procedures providing excellent filter dimensions. In the case of classic dual-mode channel filters, even the penetration depth of the screws can be accurately obtained.

It is worth pointing out that once the filter has been successfully designed, a sensitivity analysis of the resulting structure should be performed. From this analysis, the designer can determine whether to use an implementation without tuning screws or not, as well as the tolerance bound to be requested to the manufacturing process.

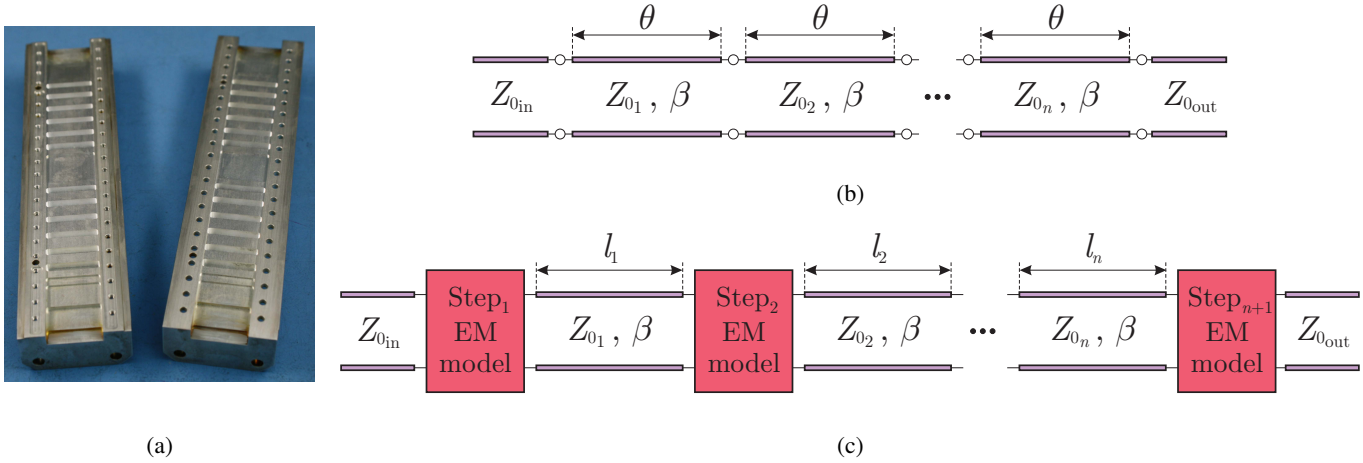

Fig. 1. Corrugated low-pass filter in rectangular waveguide and prototype representations of the structure. The classic low-pass distributed prototype is shown in (b), whereas the enhanced distributed prototype with an electromagnetic (EM) model of the waveguide steps is depicted in (c). (Photograph courtesy of Thales Alenia Space España)

II. Circuit Synthesis of Low-Pass Corrugated Waveguide Filters

Low-pass corrugated rectangular waveguide filters are an example illustrating the limitations of traditional prototype synthesis, as well as the advantages obtained from enhanced models. This topology consists of cascaded high- and low-impedance waveguide sections, as shown in Fig. 1(a). The classic distributed low-pass prototype depicted in Fig. 1(b) represents the alternation between short lengths of high- and low-impedance lines, which provide the low-pass filtering capability [4], [39]. Since this prototype can be synthesized in an analytical form, it has been used for decades in the design of this type of structure.

According to traditional techniques, a suitable Chebychev or Zolotarev response with a prescribed stopband performance is first chosen [40], [41]. The transmission line impedances Z_{0_i} and phase θ_0 at the passband upper frequency f_0 are then synthesized. Next, these prototype parameters are transferred to the waveguide heights b and lengths l by using

$$\frac{Z_{0_{i+1}}}{Z_{0_i}} = \frac{b_{i+1}}{b_i} \tag{1}$$

$$l = \frac{\theta}{\beta} = \frac{\theta_0}{\beta|_{f=f_0}} \tag{2}$$

and a commensurate structure with equal waveguide lengths l is then obtained. The expression (1) set the waveguide heights b_i once the height b_0 of the filter input waveguide has been fixed. The value of b_0 is usually chosen according to power and spurious requirements.

This simplified procedure does not provide accurate estimates for the filter dimensions, since the response of the extracted filter is not usually close to the ideal transfer function. The main source of

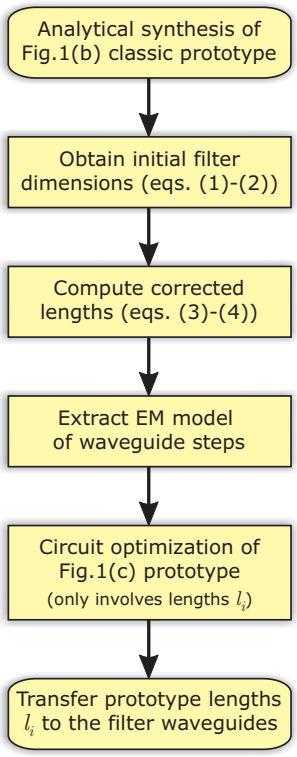

Fig. 2. Flow chart of the synthesis procedure of low-pass corrugated filters proposed in [34].

error comes from neglecting some effects of the discontinuities between adjacent waveguides. The circuit prototype models each discontinuity as a simple impedance step, whereas a more rigorous analysis adds a capacitive shunt element related to the reactive energy stored around the discontinuity [42]. The step capacitances can be obtained by use of the approximate expressions in [42], [43]. These closed form expressions can be easily computed, but they have errors of a few percent that can ultimately limit the synthesis accuracy. This limitation is avoided if EM simulators are used to extract the step capacitances, which can be efficiently computed with advanced modal analysis methods [29]. Although the CPU time required to complete the synthesis will be slightly increased, a dramatic reduction in the overall design time can be expected if the burden of the final EM optimization is reduced or even avoided.

A prototype that includes the shunt step capacitances, computed from either closed-form expressions or full-wave simulators, cannot be synthesized in an analytical form. To circumvent this problem, a modified procedure that corrects the waveguide lengths has been proposed in [17], partly based on the classic work of Levy [44] used for years by practitioners. The input and output reflection coefficients of the ideal prototype steps are real (see Fig. 1(b)). However, the shunt capacitive effect introduces a phase shift in the reflection coefficients of each single waveguide step. To equate the prototype and the structure at the passband cutoff frequency f_0, the correction lengths that compensate for these phase shifts are derived.

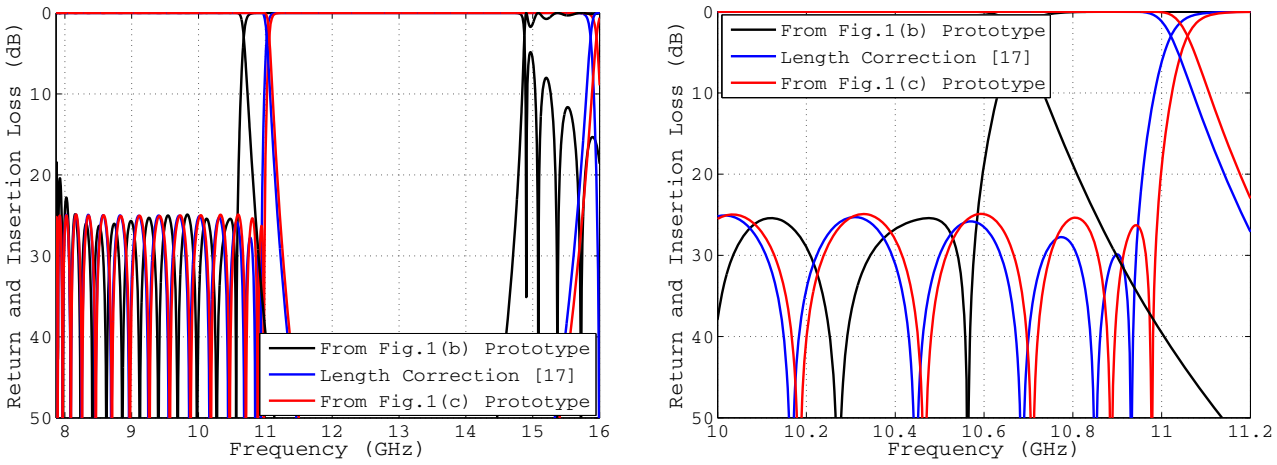

Fig. 3. Comparison of the extracted structure responses using the different synthesis techniques considered in this section. Wideband responses in (a), and detail of the responses close to the passband cutoff frequency in (b). Figures extracted with modifications from [34]. (Courtesy of the European Microwave Association, EuMA)

For the i-th structure step, such waveguide lengths are

$$\delta_i^{(j)} = \frac{\lambda_g}{4\pi}\,\phi_i^{(j)}\Big|_{f=f_0} \quad ; \quad j = 1, 2 \tag{3}$$

where $\phi_i^{(j)}$ is the phase of the reflection parameter S_{jj} of the isolated waveguide step and λ_g is the structure guide wavelength. Therefore, the length of the i-th filter waveguide section is now given by

$$l_i = l + \delta_i^{(2)} + \delta_{i+1}^{(1)} \tag{4}$$

These length corrections do improve the extracted structure and its response. However, they are merely an adjustment to the classic prototype in Fig. 1(b).

The representation of the structure can be improved if the waveguide steps are analyzed with a full-wave EM simulator and their responses are stored in the form of ABCD matrices [34]. The unconventional prototype shown in Fig. 1(c) is thus obtained. Unfortunately, the prototype response cannot be expressed in terms of a simple rational function in θ, and an analytical synthesis procedure providing the prototype lengths is unavailable. Instead, a fast circuit optimization based on the equiripple algorithm in [45] and starting from the corrected lengths (4) is performed. The flow chart of the resulting synthesis procedure is shown in Fig. 2.

To test the performance of the synthesis methods described above, a 31^{st} order low-pass corrugated filter for high-power applications has been considered [34]. The filter passband cutoff frequency f_0 was 11 GHz, with a specified return loss of 25 dB, and a gap height greater than 4.25 mm. The responses of the

different extracted structures are compared in Fig. 3. Using the distributed prototype in Fig. 1(b), which neglects the step capacitances, an important shift in the passband cutoff frequency and the filter stopband is observed. Some reflection zeros are also lost. This extracted structure is far from the final solution. After applying the length corrections (3)–(4) according to [17], a significant improvement is observed. The resulting structure, however, requires a final optimization because the filter cutoff frequency is shifted 60 MHz downwards and the upper passband ripple is slightly impaired.

Finally, the approach in [34], which uses the closest prototype to the real filter, provides the best synthesized structure. A final optimization is not required in this case because the error in the filter dimensions is below typical manufacturing tolerances. The slight deviation of the extracted structure response in Fig. 3 can be attributed to the higher-order modes, which are the only contributions ignored in the prototype in Fig. 1(c). As the waveguide lengths become shorter and/or higher waveguide sections are used, the effects of such modes increase and the synthesis accuracy is reduced. For instance, to obtain wider stopbands, the discontinuities must become closer to move the spurious passband upwards in frequency, and higher impedance sections must be used to keep the same filter gap. The prediction of the filter cutoff frequency will therefore be degraded. High-power applications with wide stopbands often require impractical waveguide sections. As a result, low-pass corrugated filters with high gaps, such as the one in the example, followed by harmonic suppressors should be used [46].

This example points out the importance of using the closest physical representation of the real filter. Traditional prototypes are simplified models able to be synthesized in an analytical form, and their extracted structures normally require some sort of correction (usually involving a cumbersome EM optimization). Using current full-wave simulation capabilities, better models including relevant second-order effects can be derived. Although a more difficult synthesis must be carried out, the resulting structure is highly improved and the burden of the final EM optimization is reduced or even avoided. The closer the model to the structure, the higher the benefits in terms of robustness and efficiency.

III. Circuit Synthesis of Wideband and Inhomogeneous Inductive Waveguide Filters

Circuit prototypes for microwave filters are generally composed of immittance inverters and resonators. To simplify the prototypes and guarantee that they may be analytically synthesized, constant immittance inverters are commonly assumed, as well as identical prototype resonators. As a result, the prototype response is a rational function in terms of a common complex frequency variable s. These approximations are valid for narrowband applications, where a constant coupling matrix completely defines the prototype

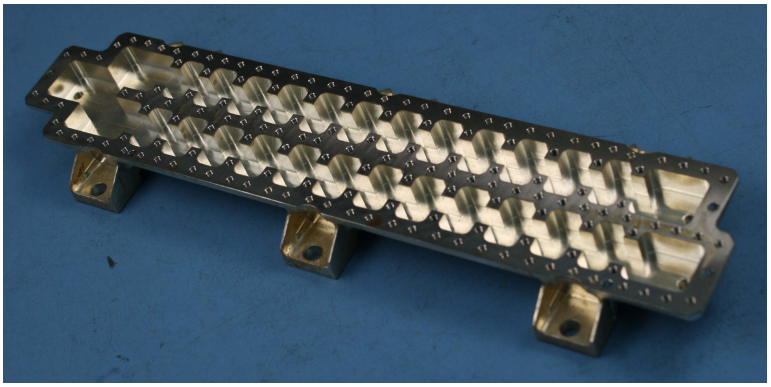

Fig. 4. Body of a diplexer composed of two inductive filters with rounded corners. (Courtesy of Thales Alenia Space España)

and the real filter behavior [5]. Exploiting the coupling matrix or equivalent schemes, very powerful synthesis and design methods of narrowband filters have been developed (see [12], [13], [15], [47] and [48] to cite a few). However, as the filter bandwidth increases, the accuracy of the previous methods is seriously reduced. In fact, they are usually unsuitable for relative bandwidths greater than 5%. Moreover, if the structure's resonators and/or coupling elements do not share the same variation with frequency (i.e., the structure is inhomogeneous), the performance of the narrowband approaches degrades even faster. In wideband and inhomogeneous applications, the frequency dependence of the real structure elements must be rigorously taken into account in the synthesis procedure. Inhomogeneous filters are of practical interest, since their additional degrees of freedom can be used to improve the filter performance [49].

In-line inductive waveguide filters have been used for decades in a wide range of practical applications (see Fig. 4). The synthesis and design of such filters have been studied in depth, achieving significant advances over Cohn's method [10], which is ultimately based on a bandpass prototype derived from lumped-elements. The most widely used methodologies are due to Levy [19] and Rhodes [11]. These techniques are essentially the same, since both are based on a distributed prototype with ideal shunt inductances as impedance inverters. The prototype elements are similar to the real structure parts, and after minor simplifications, an analytical synthesis procedure can be established. The method in [19] performs the synthesis by applying a frequency mapping to the classic distributed half-wave prototype [40], whereas the technique in [11] directly provides explicit approximate formulae for the prototype elements.

A new dimensional synthesis method has been presented in [21], which considers the diverse frequency variation of the real coupling elements by means of their slope parameters [50]. After performing an initial synthesis of the structure, the slope parameters of the extracted coupling windows are computed through EM simulations and added to the slope parameters of their adjacent resonators. These modified

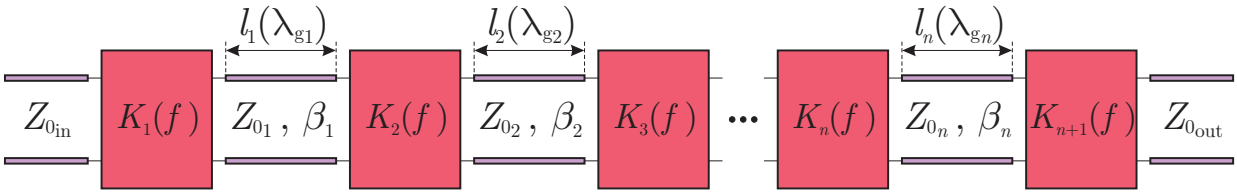

Fig. 5. Generalized prototype for in-line inductive filters able to accurately model the frequency dependence of the structure parts.

slope parameters are then used to perform an improved synthesis with a better representation of the structure around the filter's center frequency, although the accuracy of the model reduces for frequencies increasingly far from the passband center. These methods prove to be appropriate for moderate bandwidths (i.e., up to about 15% relative bandwidth in guide wavelength terms) due to the simplifications carried out for the sake of an analytically synthesizable prototype. Moreover, a common guide wavelength is used, thus making the techniques suitable only for homogeneous filters. The technique in [11] was generalized to the inhomogeneous case in [51], although the resulting method is only valid in a very narrowband regime.

A synthesis procedure similar to the one described in Section II is not possible in this case. Although the inductive irises could be divided in two cascaded discontinuities, and the length between them could be used to set the coupling, the synthesis accuracy would be compromised by the higher-order modes present in such short waveguide sections. Additionally, this technique would not be well suited to use the iris widths to control the coupling (which is the option usually preferred in practice). Hence, the coupling elements must be modeled as a whole. There is not much sense, however, in using an EM matrix representation that must be continuously recomputed during the synthesis. It is far more efficient to use a frequency variant circuit to model the real impedance inverters.

Inductive homogeneous filters in rectangular waveguide can be designed using the techniques described in [52], [53], which are able to consider the rounded corners arising from manufacturing. These techniques establish an EM-based polynomial model of a fixed-length coupling window in terms of its width and the frequency. The design procedure relies on a brute-force optimization of the structure in which the EM-based model is only used to replace the EM simulator. As a result, an important reduction of the overall design time is obtained at the cost of a slight degradation in accuracy.

A more elaborate methodology has been recently proposed to perform the synthesis of wideband and/or inhomogeneous in-line inductive filters [35], [36]. This technique is based on the generalized prototype in Fig. 5. The propagation constant β_i and guide wavelength λ_{g_i} of the fundamental mode of the i-th

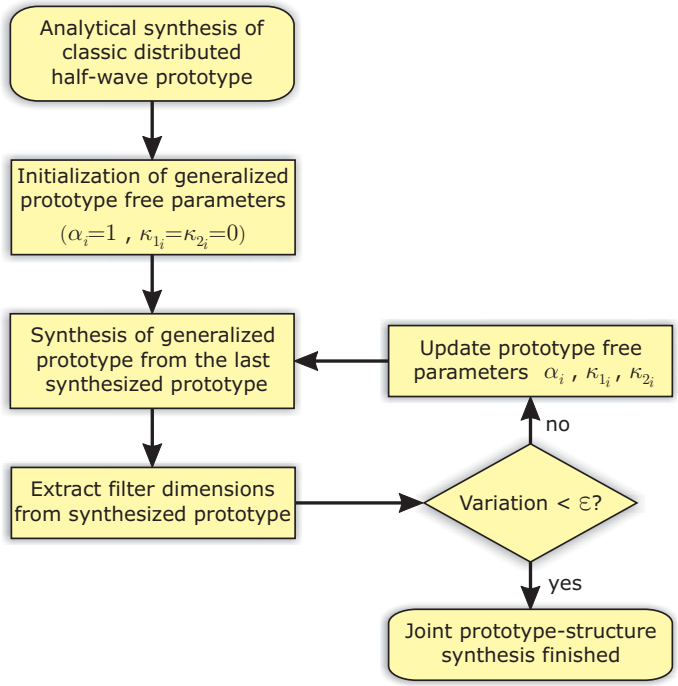

Fig. 6. Flow chart of the synthesis procedure for bandpass filters proposed in [35], [36].

structure resonator are used in its corresponding prototype line, whereas the line characteristic impedance is

$$Z_{0_i} = \eta \left(\frac{\lambda_{\mathrm{g}_i}}{\lambda} \right)^{\gamma_i} \tag{5}$$

η the intrinsic impedance of the medium and γ_i a parameter used to control the frequency dependence of the prototype characteristic impedances, which is normally set to 1 to represent a TE mode.

The inductive obstacles are accurately represented by means of frequency variant impedance inverters and transmission line lengths (which absorb the frequency dependence of the correction lengths that must be added to the structure obstacles to behave as pure inverters). After transferring such lengths to the adjacent resonators, the prototype impedance inverter parameters and transmission line lengths are

$$K_i(f) = K_{0_i} \left(\frac{f}{f_{0_{\mathrm{inv}}}} \right)^{\alpha_i} \tag{6a}$$

$$l_i(\lambda_{\mathrm{g}_i}) = \frac{\lambda_{\mathrm{g}0_i}}{2} + \kappa_{1_i} \left(\frac{1}{\lambda_{\mathrm{g}_i}} - \frac{1}{\lambda_{\mathrm{g}0_i}} \right) + \kappa_{2_i} \left(\frac{1}{\lambda_{\mathrm{g}_i}} - \frac{1}{\lambda_{\mathrm{g}0_i}} \right)^2 \tag{6b}$$

where K_{0_i} is the impedance parameter of the i-th inverter at $f_{0_{\mathrm{inv}}}$ (an arbitrary reference frequency), and $\lambda_{\mathrm{g}0_i}$ is the guide wavelength λ_{g_i} of the i-th resonator at its resonant frequency f_{0_i}. The prototype's free parameters α_i, κ_{1_i} and κ_{2_i} are used to match the structure behavior over a wide frequency range. Unfortunately, the free parameters of the prototype depend on the structure's dimensions, which usually

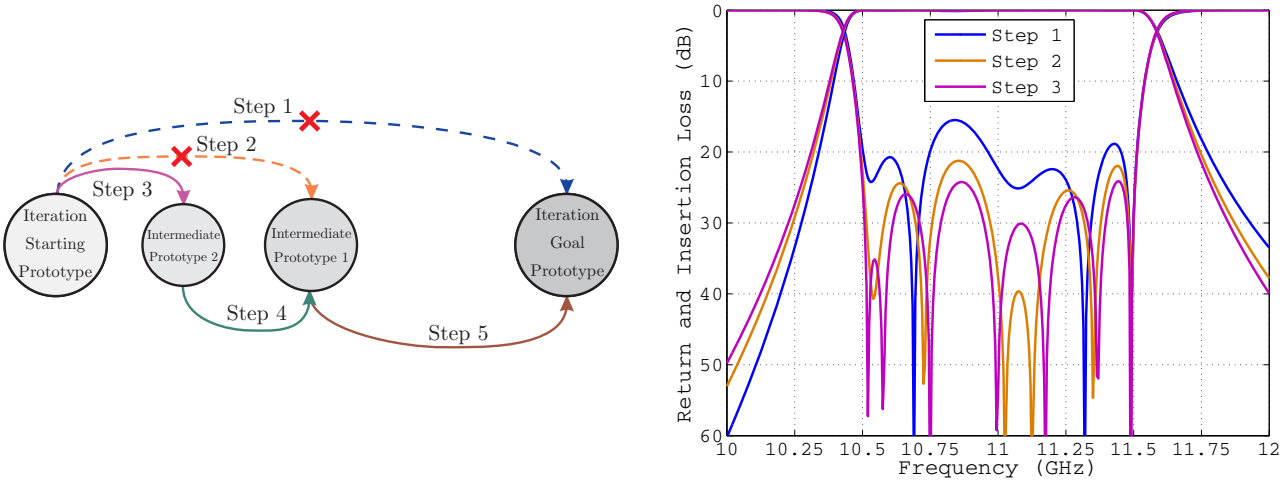

(a) (b)

Fig. 7. Schematic description of a synthesis method iteration in (a) according to [35] (the dashed and continuous lines denote aborted and succesful steps, respectively). Prototype responses after the analytical approximate synthesis procedure in the first three steps in (b).

change during the synthesis. An iterative synthesis procedure is thus followed, whose flow chart is depicted in Fig. 6.

The procedure starts with the analytical synthesis of the classic distributed half-wave prototype. This homogeneous prototype is a particular case of the generalized prototype in Fig. 5 with the parameters γ_i, α_i, κ_{1_i} and κ_{2_i} set to 0 and the same common guide wavelength in all of the transmission lines. Next, the synthesis of a generalized prototype with $\gamma_i = 1$, $\alpha_i = 1$ and $\kappa_{1_i} = \kappa_{2_i} = 0$ is carried out before the first structure extraction. This prototype models a waveguide filter with ideal shunt inductive obstacles, and includes the real frequency behavior of the different structure resonators. From the synthesized prototype, the dimensions of the filter parts are then extracted, and the prototype parameters α_i, κ_{1_i} and κ_{2_i} are updated to acquire the wideband behavior of the new coupling windows. Since this update changes the prototype, it must be synthesized again and a new iteration starts. The combined prototype-structure synthesis finishes once the maximum variation in the physical dimensions of two consecutive extracted structures is below a convergence bound ϵ.

To guarantee success of this methodology, the ideal transfer function must always be recovered with the synthesized prototypes. The prototype synthesis starts from the final prototype of the last iteration, and aims to obtain the parameters f_{0_i} and K_{0_i} of the new prototype updated with the frequency dependence of the last extracted filter (inhomogeneous structures are asynchronously tuned devices, so different f_{0_i} can be obtained). Since the prototype cannot be synthesized in an analytical form, an approximate synthesis procedure followed by a fast circuit optimization is performed [35]. If a cumbersome circuit optimization

is detected (i.e., the starting point is not good enough), the prototype flexibility is fully exploited. An intermediate prototype midway between the starting and the goal prototype is created. The algorithm then tries to synthesize the intermediate prototype instead of the goal. Once the intermediate prototype has been synthesized, it is used to obtain the goal prototype. The strategy is recursive, since additional intermediate prototypes can be created as required. Fig. 7 illustrates a prototype synthesis involving intermediate prototypes.

Finally, the extraction of the filter dimensions is based on the relationship between the reflection coefficient S_{11} of a coupling window and the parameter K of their equivalent impedance inverter

$$\frac{K\left(f\right)}{\sqrt{Z_{0_{\text{in}}}\left(f\right)Z_{0_{\text{out}}}\left(f\right)}}=\sqrt{\frac{1-\left|S_{11}\left(f\right)\right|}{1+\left|S_{11}\left(f\right)\right|}} \tag{7}$$

which allows use of a root-finding method to determine the iris dimensions that provide the inverter parameter K at $f_{0_{\text{inv}}}$ of the synthesized prototype. A correction length must also be added to the input and output waveguides of each coupling element to obtain the ± 90 degree phase shift of an ideal impedance inverter, namely

$$l_{\text{in}}\left(f\right)=\frac{1}{\beta_{\text{in}}\left(f\right)}\left(\frac{\phi_{11}\left(f\right)}{2}+\frac{\left(2n-1\right)\pi}{2}\right) \tag{8a}$$

$$l_{\text{out}}\left(f\right)=\frac{1}{\beta_{\text{out}}\left(f\right)}\left(\phi_{21}\left(f\right)-\frac{\phi_{11}\left(f\right)}{2}+m\pi\right) \tag{8b}$$

where n and m are integers (normally set to obtain the shortest correction lengths in magnitude), and $\phi_{11}\left(f\right)$ and $\phi_{21}\left(f\right)$ are the phase of the S_{11} and S_{21} reflection coefficients, respectively. The length of each waveguide resonator is thus obtained by adding the correction lengths of its adjacent coupling windows to half guide wavelength at its computed f_{0_i} resonant frequency.

Once the coupling windows have been extracted, their equivalent impedance parameters $K\left(f\right)$ and correction lengths $l_{\text{in}}\left(f\right)$ and $l_{\text{out}}\left(f\right)$ are derived from EM simulations (see (7)–(8)). The prototype's free parameters α_i, κ_{1_i} and κ_{2_i} are then obtained by means of a least-square fit in the form (6).

Figure 8 compares the homogeneous structures extracted with different synthesis methods for a 6^{th} order moderate bandwidth filter and the wideband 11^{th} order filter in [35]. The methods in [11] and [19] provide nearly the same results, which are comparable to the ones obtained by the more recent method in [21]. Although the extracted structures exhibit a good response, Fig. 8(a) shows some degradation in the bandwidth and return loss level. These impairments increase in the wideband filter, with four of the eleven reflection zeros placed out of the frequency axis (see Fig. 8(b)). The method in [35] yields outstanding filter responses in both cases, at the expense of a more intricate but precise synthesis procedure. The

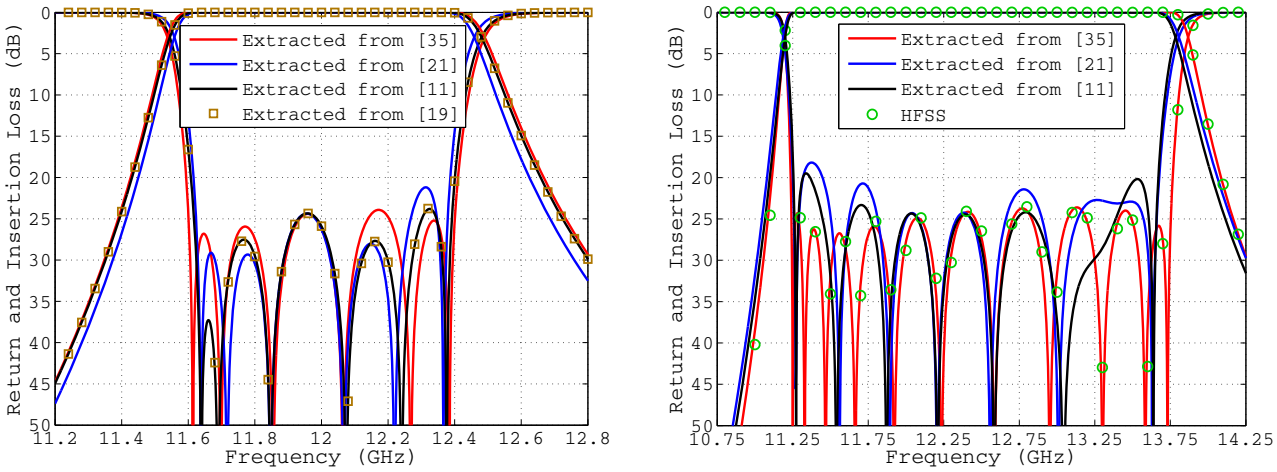

(a) (b)

Fig. 8. Comparison between the responses of the extracted structures with different synthesis methods for two WR75 homogeneous inductive waveguide filters with 25 dB return loss. In (a) a 800 MHz moderate bandwidth filter (11.7% guide wavelength relative bandwidth) and in (b) a 2.5 GHz wide bandwidth filter (33.2% guide wavelength relative bandwidth) [35]. For verification purposes, the response obtained in (b) with the accurate method of [35] has also been simulated with HFSS [54].

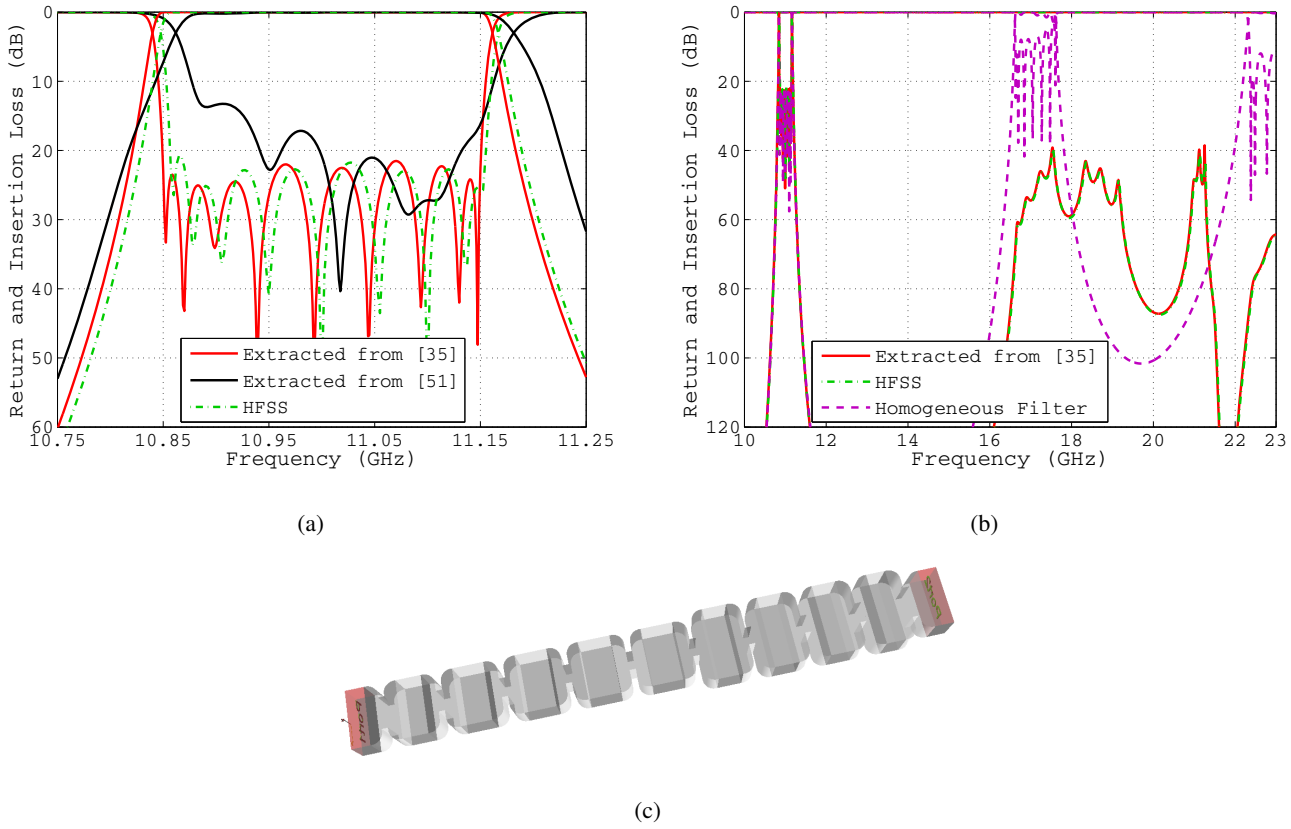

(a) (b)

(c)

Fig. 9. Passband in (a) and stopband in (b) responses of the synthesized inhomogeneous filter with rounded corners. The structure layout is plotted in (c).

CPU time required by all the methods is below 1 second. From Monte Carlo analyses performed on equal ripple optimized filters, it can be concluded that the impairments in the responses obtained from the techniques [11], [19] and [21] are equivalent to a manufacturing tolerance of $\pm$25–100 μm (mainly due to the bandwidth shrinkage). Using the technique in [35], only a 1.3 dB reduction in the return loss ripple is observed in both filters, which corresponds to the expected degradation of a manufacturing tolerance slightly below ± 5 μm.

For the last example, a 9^{th} order inhomogeneous filter with inductive coupling windows and rounded corner resonators has also been synthesized. The passband was centered at 11 GHz, with 23 dB return loss and 300 MHz bandwidth. The non-equal resonator widths were carefully chosen to provide at least a 2:1 stopband range. The filter passband and wideband responses are shown in Fig. 9. The response of the structure extracted from [51] shows the limitations of this technique, with errors in several physical dimensions greater than 500 μm (which are difficult to be restored after a long and cumbersome EM optimization). On the other hand, the results from [35] only show small variations in the passband ripple level (about ± 1.5 dB), which are due to the higher-order modes not included in the prototype. Furthermore, very good agreement with HFSS data is also observed. The small frequency shift of about 0.06% can be attributed to the HFSS linear segmentation of the rounded corners [54], which replaces circular contours with circumscribed polygons and reduces the surface of the waveguide resonators. The synthesis took 2 minutes. The final EM optimization is also avoided in this asymmetric filter with a sensitivity figure below ± 5 μm, which probably will require tuning screws to compensate for manufacturing tolerances.

IV. Equivalent Distributed Circuit Models for the Systematic Design Procedure of Narrowband Bandpass Waveguide Filters

Although classic lumped-element circuits can implement any coupling matrix, and therefore provide the electrical response of any narrowband filter, the use of prototypes closer to the real structure can also be advantageous in the narrowband case. Using such prototypes, a clear correspondence between the structure parts and the prototype elements can be identified. This correspondence can be exploited to establish a more precise synthesis procedure able to extract an improved structure. Two widely used types of filters are discussed in this section. In both cases, a distributed prototype is used to represent the structure. Although these prototypes can model the component over wider bandwidths, they are synthesized following Cohn's classic procedure [10]. This simple approach is effective because the filters under consideration are narrowband.

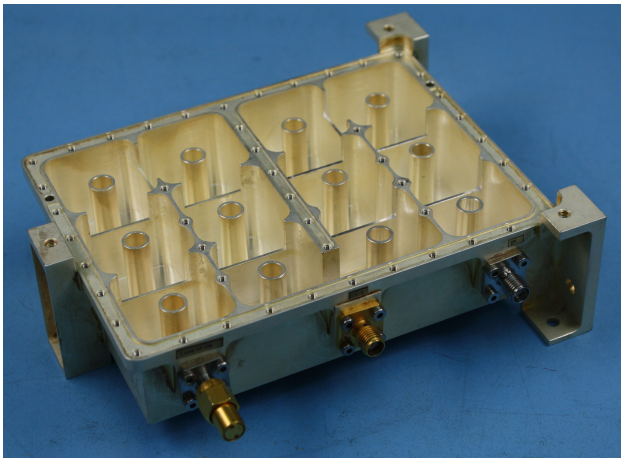

Fig. 10. A coaxial diplexer with combline resonators coupled by small lateral apertures. (Courtesy of Thales Alenia Space España)

A. Side Coupled In-Line Coaxial Cavity Filters

Coaxial cavity filters coupled by small lateral apertures are extensively used in practical narrowband applications due to their compact size, good quality factor and good spurious performance (see Fig. 10). The synthesis methods for direct-coupled cavity filters [10] are not well-suited for side coupling, whereas the classic techniques for combline and interdigital filters assume proximity coupling, which is appropriate for moderate and wide bandwidths [55]. To obtain the initial filter dimensions, however, a direct-coupled cavity prototype form with shunt stub resonators is normally used [4]. The side couplings are usually set by means of an even/odd analysis of a symmetric or asymmetric pair of coaxial resonators [56], [57], that can be efficiently performed with advanced modal methods as described in [57]. Although the synthesized dimensions are not far from the final solution, the structure response is usually poor due to the filter sensitivity and the approximations carried out, and it should be improved with the help of computer optimization. Eventually, the ideal transfer function is always restored with tuning screws, included to compensate for the manufacturing tolerances in such sensitive narrowband filters.

A new design method without EM optimization was recently presented in [37], [58]. For the configuration with the coupling apertures placed on the side opposite the end gaps (see Fig. 11(b)), the prototype in Fig. 11(a) has been proposed. This prototype includes shunt capacitances to represent the resonator end gaps, and series inductances to model the phase shifts due to the real coupling elements and the filter ports. Once the parameters L_i and C_i are known, the prototype can be analytically synthesized from the direct-coupled cavity filter after performing some circuit transformations and narrowband approximations. Next, a new structure implementing the synthesized prototype is extracted. This update of the filter dimensions, however, changes the structure dependent parameters L_i and C_i and modifies the prototype that must be

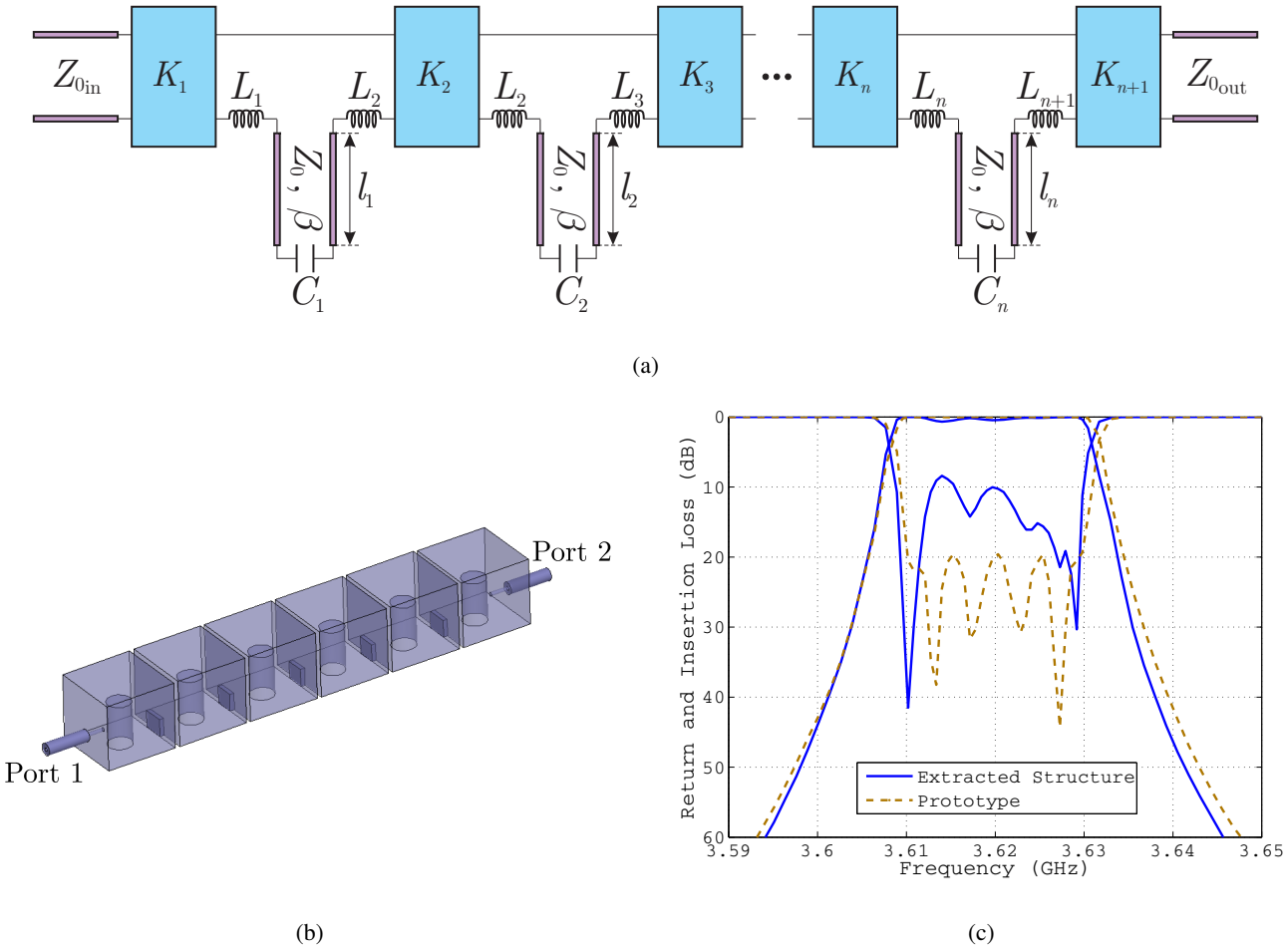

Fig. 11. Prototype for in-line side-coupled coaxial cavity filters in (a), whose topology is depicted in (b). Comparison between the extracted structure and the synthesized prototype for the 20 MHz bandwidth filter in (c) (data extracted from Fig. 11 in [58]).

synthesized again in a new iteration. A combined prototype-structure synthesis procedure similar to the one described in Section III is thus obtained (although the prototype is analytically synthesized in this narrowband case).

The results for the 6^{th} order in-line coaxial filter described in [58] are depicted in Fig. 11(c). Even though the specified passband return loss level is not exactly recovered, the extracted structure response is very good when compared to classic methods (see Fig. 14 in [58]). An outstanding initial guess of the filter is obtained without costly EM optimizations, which allows one to set the dimensions of the device to be manufactured. The response is finally compensated with the tuning elements always included in these sensitive filters.

B. Dual-Mode Circular Waveguide Filters

Since the 1970s, dual-mode waveguide filters have been widely used in satellite hardware, due to their reduced mass and volume features [59]–[61]. Using two orthogonal degenerate modes inside each cavity,

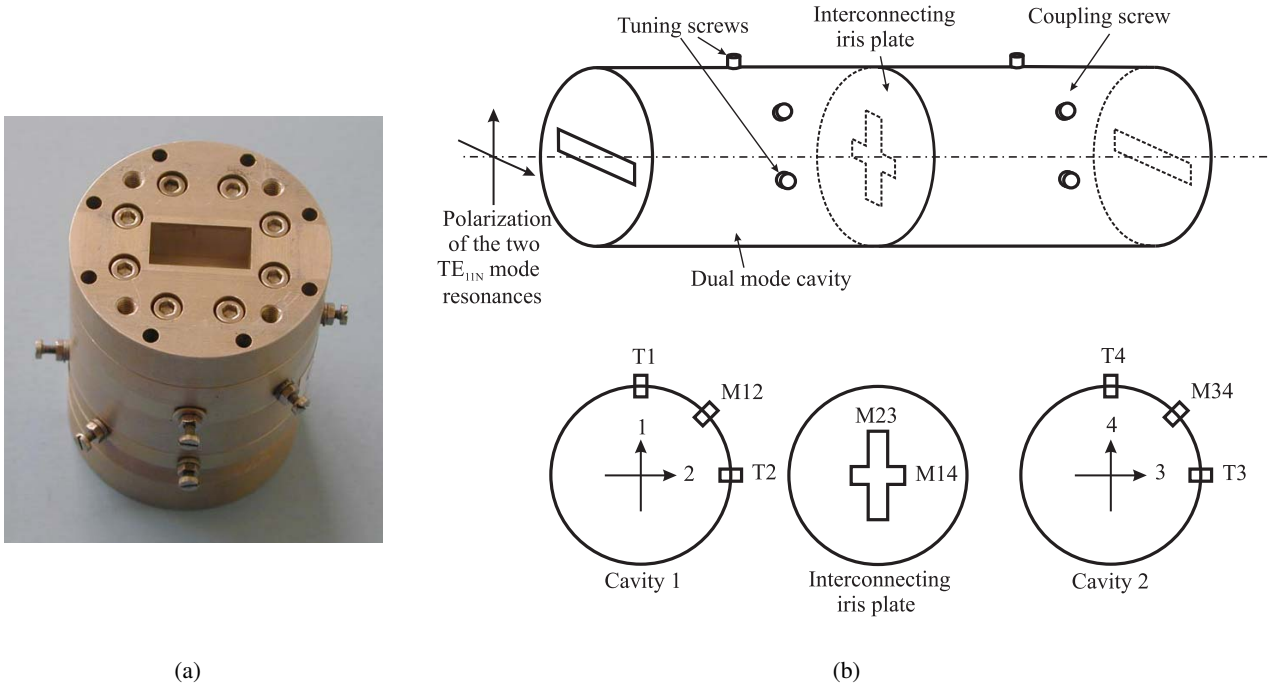

(a) (b)

Fig. 12. Classic configuration of a 4th order dual-mode filter in circular waveguide. Assembled filter in (a). Schematic description of the filter parts in (b).

an N-pole filter can be implemented with only $N/2$ cavities. Additionally, transmission zeros can be easily obtained with in-line topologies, thus allowing these compact structures to be assembled within satellite platforms. Circular waveguide topologies provide higher quality factors than their rectangular counterparts [22], [62], and are preferred for space applications. Since very narrow bandwidths are typically specified, the filter sensitivity is usually below manufacturing tolerances. As a result, tuner-less implementations [63] are commonly avoided.

The classic dual-mode filter configuration normally used in practice is shown in Fig. 12, which includes three screws on each dual-mode cavity. The vertical and horizontal screws (so-called tuning screws) are used for the fine adjustment of the center frequency of each polarization. The diagonal (or coupling) screw controls the degree of interaction between the two degenerated modes in the same cavity. The iris placed between the two adjacent cavities is cross-shaped. The vertical arm of the cross couples the horizontal modes of both cavities, whereas the horizontal arm does the same for the vertically polarized modes.

The design of dual-mode circular waveguide filters has been traditionally carried out with theoretical curves, empirical data and brute-force approaches. A systematic design procedure was proposed in [64] based on the well-known, generalized, direct-coupled cavity prototype [20]. This technique is limited to narrow bandwidths. Moreover, the procedure to extract the filter dimensions does not consider second-order effects, such as the iris end-loading effects on the screws. As a result, good initial dimensions are obtained,

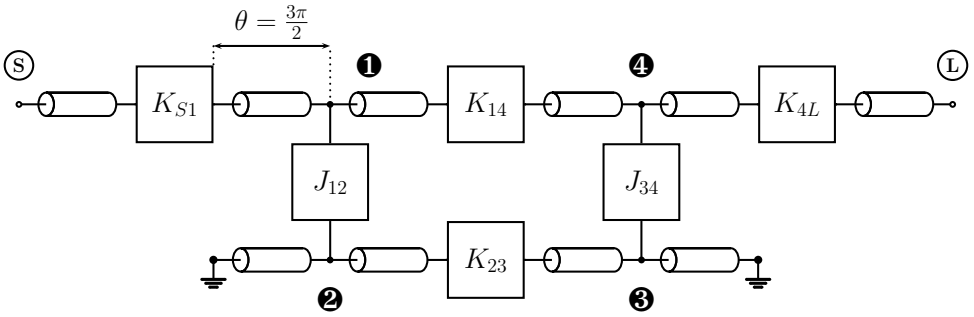

Fig. 13. Distributed model for the dual-mode configuration shown in Fig. 12.

but a time consuming EM refinement is required. Further improvement can be achieved with the help of the distributed model derived in [38] (see Fig. 13), which is a very accurate representation of the dual-mode filter in Fig. 12. This prototype is more accurate than a lumped-element network for wider bandwidths and also provides valuable information for deriving physical dimensions. Vertical modes (assuming the reference orientation of Fig. 12(b)) are driven through the upper part of the model (resonances 1 and 4), and horizontal modes are propagated through the lower part (resonances 2 and 3). The K inverters model the irises, whereas the J inverters represent the coupling screws. According to [38], the normalized formulas for the inverters shown in Fig. 13 are as follows

$$\bar{K}_{S1} = M_{S1}\sqrt{\frac{3\pi}{2}\mathcal{W}}; \quad \bar{K}_{4L} = M_{4L}\sqrt{\frac{3\pi}{2}\mathcal{W}} \tag{9a}$$

$$\bar{J}_{12} = M_{12}\frac{3\pi}{2}\mathcal{W}; \quad \bar{J}_{34} = M_{34}\frac{3\pi}{2}\mathcal{W} \tag{9b}$$

$$\bar{K}_{14} = M_{14}\frac{3\pi}{2}\mathcal{W}; \quad \bar{K}_{23} = M_{23}\frac{3\pi}{2}\mathcal{W} \tag{9c}$$

where M_{ij} are the values of the coupling matrix and $\mathcal{W} = \Delta\omega/\omega$ is the fractional bandwidth. In waveguide technology, $\mathcal{W}$ should be replaced with $\mathcal{W}_\lambda$ (fractional guide wavelength bandwidth) to take into account the dispersion characteristics of the waveguide modes

$$\mathcal{W} = \frac{\omega_2 - \omega_1}{\omega_0}; \quad \mathcal{W}_\lambda = \frac{\lambda_{g1} - \lambda_{g2}}{\lambda_{g0}} \tag{10}$$

with ω_1, ω_2 being the classic band edge frequencies, and λ_{g1}, λ_{g2} the corresponding guide wavelengths, as described in [4].

The distributed model can easily consider any resonant mode. The most widely used are the TE_{113} modes, but if higher quality factors are needed, the cavities can be enlarged to use higher TE_{11N} resonances. The only change is the position of the J-inverters (inter-resonator couplings) since their best placement is in the maximum of the electric field. At the end, formulas like (9) with $N\pi/2$ constants will arise.

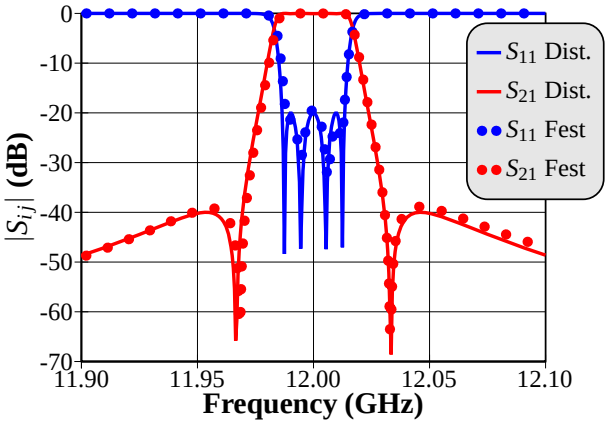

Fig. 14. Electrical response of the EM model given by FEST3D [26] compared with the distributed model response.

From the synthesized prototype, a CAD procedure can be applied to extract the dual-mode structure. The iris dimensions are derived by performing EM simulations of the isolated irises. Following the technique described in Section III, a search algorithm is used to change the iris width/height until the normalized $\bar{K}$ of the corresponding prototype inverter is obtained. The resulting irises provide different length corrections for the degenerate modes of each resonant cavity. Since the cavity has the same physical length for both modes, tuning screws are required to compensate for this effect. The penetration depths of the two tuning screws are independently adjusted to center the simulated response of each mode at the passband center frequency. On the other hand, the diagonal (coupling) screws are tuned to match the simulated response of each cavity (including its irises) with the response of the equivalent part of the prototype circuit. At each step of this CAD procedure, only one parameter has to be changed. In contrast to other methods described in this paper, an iterative prototype-structure synthesis algorithm is not needed. Exploiting the one-to-one correspondence between prototype and structure elements, a simple, fast and robust methodology can be carried out to obtain the ideal prototype response with the real filter.

Fig. 14 shows the EM simulation data of the extracted structure compared to the electrical response of the distributed model for a four-pole dual-mode filter. Note that the agreement between the distributed model and the extracted structure is excellent in the simulated bandwidth. A final optimization has not been required, and the total CPU design time has been around ten minutes on a personal computer. The final dimensions of the designed dual-mode filter are reported in Table I (cavity lengths and screw penetrations) and Table II (iris widths W and heights H), where subscripts H and V stand for “horizontal” and “vertical” respectively.

TABLE I

EXAMPLE OF ORDER $N = 4$. PHYSICAL DIMENSIONS OF CAVITIES AND PENETRATION DEPTHS OF SCREWS ON EACH CAVITY.

ALL DIMENSIONS ARE IN MM.

i	Length of cavity i	penetration depth
1	$L_1 = 54.4372$	$d_V = 1.0000$ $d_H = 2.9024$ $d_{45^\circ} = 2.032$
2	$L_2 = 54.4416$	$d_V = 1.0000$ $d_H = 2.8988$ $d_{-45^\circ} = 1.9417$

TABLE II

EXAMPLE OF ORDER $N = 4$. PHYSICAL DIMENSIONS FOR THE FILTER IRISES.

IRIS	Dimensions (mm)
Input horizontal iris	$W = 2.0000$ $H = 10.6449$
Cruciform iris between cavities 1 and 2	$W_V = 1.0000$ $L_V = 7.8276$ $W_H = 1.0000$ $L_H = 4.4191$
Output horizontal iris	$W = 2.0000$ $H = 10.6449$

V. CONCLUSIONS

Most of the circuit prototypes used in practical applications were proposed many decades ago, when the present computational resources were not available. Simplicity was a key factor in their conception. Although these traditional prototypes model the real structures, they usually neglect second-order effects, the frequency dependence of the filter parts and, in some cases, they do not have an exact correspondence with the physical structure. All of these inaccuracies can affect the equivalence between the prototype and the real filter, thus degrading the initial structure extracted from the synthesized prototype. Optimizations carried out from poor initial dimensions are computationally burdensome, and more liable to provide a filter with unsatisfactory response.

The synthesis methods reviewed in this paper are based on prototypes designed to faithfully represent the real components. These prototypes include elements to model the relevant effects of the structure in the particular designs to be carried out. Moreover, accurate EM simulators are used to find an almost exact

equivalence between the prototype and the filter parts. Although more elaborate synthesis techniques are usually required, these enhanced prototypes and synthesis procedures can be used to extract outstanding initial structures. The design is essentially solved after the dimensional synthesis of the component since, at most, only a slight and fast final refinement is needed (using an EM optimizer or the tuning elements included in narrowband filters). The examples shown in this paper reveal the capabilities of these methods to overcome the limitations of classic circuit synthesis.

ACKNOWLEDGMENTS

The authors would like to thank the staff members of Aurora Software and Testing S.L. (Valencia, Spain), for their help and support with the integration of the synthesis algorithms described in this paper within the commercial software tool FEST3D, as well as to Dr. Marco Guglielmi (from ESTEC-ESA, European Space Agency) for his contributions to the equivalent circuit modeling of dual-mode filters in circular waveguide technology. They also want to explicitly acknowledge their Master and Ph.D. students at Technical University of Valencia (in particular to Mrs. Eva Tarín, Mr. Oscar Monerris, Mrs. María Brumos and Mr. Carlos Carceller), who have contributed with several algorithm implementations and results shown in this paper.

The authors are also very grateful to Thales Alenia Space España, Madrid, Spain, for the photographs of the microwave devices shown in this paper.

REFERENCES

[1] C. Kudsia, R. J. Cameron, and W.-C. Tang, "Innovations in microwave filters and multiplexing networks for communications satellite systems," *IEEE Trans. Microwave Theory Tech.*, vol. 40, no. 6, pp. 1133–1149, Jun. 1992.

[2] J. Uher, J. Bornemann, and U. Rosenberg, *Waveguide Components for Antenna Feed Systems: Theory and CAD*. Norwood, MA: Artech House, 1993.

[3] P. Jarry and J. Beneat, *Advanced Design Techniques and Realizations of Microwave and RF Filters*. Hoboken, NJ: Wiley- IEEE Press, 2008.

[4] G. Matthaei, L. Young, and E. M. T. Jones, *Microwave Filters, Impedance-Matching Networks, and Coupling Structures*. Norwood, MA: Artech House, 1980.

[5] R. J. Cameron, C. M. Kudsia, and R. R. Mansour, *Microwave Filters for Communication Systems: Fudamentals, Design and Applications*. Hoboken, NJ: John Wiley & Sons, 2007.

[6] I. Hunter, *Theory and Design of Microwave Filters*. Cambridge: IET, 2006.

[7] J.-S. Hong and M. J. Lancaster, *Microstrip Filters for RF/Microwave Applications*. New York, NY: John Wiley & Sons, 2001.

[8] R. Levy and S. Cohn, "A history of microwave filter research, design, and development," *IEEE Trans. Microwave Theory Tech.*, vol. 32, no. 9, pp. 1055–1067, Sep. 1984.

[9] R. Levy, R. V. Snyder, and G. Matthaei, "Design of microwave filters," *IEEE Trans. Microwave Theory Tech.*, vol. 50, no. 3, pp. 783–793, Mar. 2002.

[10] S. B. Cohn, "Direct-coupled-resonator filters," *Proc. IRE*, vol. 45, no. 2, pp. 187–196, Feb. 1957.

[11] J. D. Rhodes, *Theory of Electrical Filters*. John Wiley & Sons, 1976.

[12] S. Bila, D. Baillargeat, M. Aubourg, S. Verdeyme, P. Guillon, F. Seyfert, J. Grimm, L. Baratchart, C. Zanchi, and J. Sombrin, "Direct electromagnetic optimization of microwave filters," *IEEE Microw. Mag.*, vol. 2, no. 1, pp. 46–51, Mar. 2001.

[13] S. F. Peik and R. R. Mansour, "A novel design approach for microwave planar filters," in *IEEE MTT-S Int. Microwave Symp. Dig.*, Seattle, WA, Jun. 2002, pp. 1109–1112.

[14] P. Kozakowski and M. Mrozowski, "Automated CAD of coupled resonator filters," *IEEE Microwave Wireless Compon. Lett.*, vol. 12, no. 12, pp. 470–472, Dec. 2002.

[15] A. Garcia-Lamperez, S. Llorente-Romano, M. Salazar-Palma, and T. K. Sarkar, "Efficient electromagnetic optimization of microwave filters and multiplexers using rational models," *IEEE Trans. Microwave Theory Tech.*, vol. 52, no. 2, pp. 508–521, Feb. 2004.

[16] J. V. Morro, P. Soto, H. Esteban, V. E. Boria, C. Bachiller, M. Taroncher, S. Cogollos, and B. Gimeno, "Fast automated design of waveguide filters using aggressive space mapping with a new segmentation strategy and a hybrid optimization algorithm," *IEEE Trans. Microwave Theory Tech.*, vol. 53, no. 4, pp. 1130–1142, Apr. 2005.

[17] M. Simeoni, S. Cacchione, F. Vanin, J. Molina, and D. Schmitt, "Automatic dimensional synthesis without optimization for stepped impedance low-pass filters," *Microw. Opt. Techn. Lett.*, vol. 44, no. 2, pp. 190–194, Jan. 2005.

[18] L. Young, "Direct-coupled cavity filters for wide and narrow bandwidths," *IEEE Trans. Microwave Theory Tech.*, vol. 11, no. 3, pp. 162–178, May 1963.

[19] R. Levy, "Theory of direct-coupled-cavity filters," *IEEE Trans. Microwave Theory Tech.*, vol. 15, no. 6, pp. 340–348, Jun. 1967.

[20] J. D. Rhodes, "The generalized direct-coupled cavity linear phase filter," *IEEE Trans. Microwave Theory Tech.*, vol. 18, no. 6, pp. 308–313, Feb. 1970.

[21] F. M. Vanin, D. Schmitt, and R. Levy, "Dimensional synthesis for wide-band waveguide filters and diplexers," *IEEE Trans. Microwave Theory Tech.*, vol. 52, no. 11, pp. 2488–2495, Nov. 2004.

[22] P. Savi, D. Trinchero, R. Tascone, and R. Orta, "A new approach to the design of dual-mode rectangular waveguide filters with distributed coupling," *IEEE Trans. Microwave Theory Tech.*, vol. 45, no. 2, pp. 221–228, Feb. 1997.

[23] A. Lapidus, "Circuit simulation of dual-mode waveguide cavity filters," *Microw. J.*, vol. 51, no. 11, pp. 70–78, Nov. 2008.

[24] M. Bekheit and S. Amari, "A direct design technique for dual-mode inline microwave bandpass filters," *IEEE Trans. Microwave Theory Tech.*, vol. 57, no. 9, pp. 2193–2202, Sep. 2009.

[25] A. Morini, G. Venanzoni, T. Rozzi, and M. Villa, "A new prototype for the design of side-coupled coaxial filters with close correspondence to the physical structure," in *Proc. 35th Eur. Microwave Conf.*, Paris, France, Oct. 2005, pp. 413–416.

[26] *FEST3D 6.6.0*, Aurora Software and Testing, S.L. on behalf of ESA/ESTEC, Valencia, Spain, www.fest3d.com.

[27] G. Conciauro, M. Guglielmi, and R. Sorrentino, *Advanced Modal Analysis: CAD Techniques for Waveguide Components*. New York, NY: John Wiley & Sons, 2000.

[28] M. Guglielmi, G. Gheri, M. Calamia, and G. Pelosi, "Rigorous multimode network numerical representation of inductive step," *IEEE Trans. Microwave Theory Tech.*, vol. 42, no. 2, pp. 317–326, Feb. 1994.

[29] M. Guglielmi and G. Gheri, "Rigorous multimode network numerical representation of capacitive steps," *IEEE Trans. Microwave Theory Tech.*, vol. 42, no. 4, pp. 622–628, Apr. 1994.

[30] G. Gerini, M. Guglielmi, and G. Lastoria, "Efficient integral equation formulations for admittance or impedance representation of planar waveguide junctions," in *IEEE MTT-S Int. Microwave Symp. Dig.*, Baltimore, MD, Jun. 1998, pp. 1747–1750.

[31] K. Kurokawa, "The expansions of electromagnetic fields in cavities," *IRE Trans. Microw. Theory Tech.*, vol. 6, no. 2, pp. 178–187, Apr. 1957.

[32] G. Conciauro, M. Bressan, and C. Zuffada, "Waveguide modes via an integral equation leading to a linear matrix eigenvalue problem," *IEEE Trans. Microwave Theory Tech.*, vol. 32, no. 11, pp. 1495–1504, Nov. 1984.

[33] P. Arcioni, M. Bressan, and L. Perregrini, "A new boundary integral approach to the determination of the resonant modes of arbitrarily shaped cavities," *IEEE Trans. Microwave Theory Tech.*, vol. 43, no. 8, pp. 1848–1855, Aug. 1995.

[34] O. Monerris, P. Soto, S. Cogollos, V. E. Boria, J. Gil, C. Vicente, and B. Gimeno, "Accurate circuit synthesis of low-pass corrugated waveguide filters," in *Proc. 40th Eur. Microwave Conf.*, Paris, France, Oct. 2010, pp. 1237–1240.

[35] P. Soto, E. Tarín, V. E. Boria, C. Vicente, J. Gil, and B. Gimeno, "Accurate synthesis and design of wideband inhomogeneous inductive waveguide filters," *IEEE Trans. Microwave Theory Tech.*, vol. 58, no. 8, pp. 2220–2230, Aug. 2010.

[36] P. Soto and V. E. Boria, "A versatile prototype for the accurate design of homogeneous and inhomogeneous wide bandwidth direct-coupled-cavity filters," in *IEEE MTT-S Int. Microwave Symp. Dig.*, Fort Worth, TX, Jun. 2004, pp. 451–454.

[37] A. Morini, G. Venanzoni, and T. Rozzi, "A new adaptive prototype for the design of side-coupled coaxial filters with close correspondence to the physical structure," *IEEE Trans. Microwave Theory Tech.*, vol. 54, no. 3, pp. 1146–1153, Mar. 2006.

[38] S. Cogollos, M. Brumos, V. E. Boria, C. Vicente, B. Gimeno, and M. Guglielmi, "New distributed model for synthesis of classical dual mode filters," in *IEEE MTT-S Int. Microwave Symp. Dig.*, vol. 1, Anaheim, CA, May 2010, pp. 437–440.

[39] D. M. Pozar, *Microwave Engineering*, 3rd ed. New York, NY: John Wiley & Sons, 2005.

[40] R. Levy, "Tables of element values for the distributed low-pass prototype filter," *IEEE Trans. Microwave Theory Tech.*, vol. 13, no. 5, pp. 514–536, Sep. 1965.

[41] ——, "Generalized rational function approximation in finite intervals using Zolotarev functions," *IEEE Trans. Microwave Theory Tech.*, vol. 18, no. 12, pp. 1052–1064, Dec. 1970.

[42] L. Lewin, *Advanced Theory of Waveguides*. London: Iliffe & Sons, 1951.

[43] N. Marcuvitz, *Waveguide Handbook*. London: IET, 1986.

[44] R. Levy, "Tapered corrugated waveguide low-pass filters," *IEEE Trans. Microwave Theory Tech.*, vol. 21, no. 8, pp. 526–532, Aug. 1973.

[45] D. Budimir, *Generalized Filter Design by Computer Optimization*. Norwood, MA: Artech House, 1998.

[46] I. Arregui, I. Arnedo, A. Lujambio, M. Chudzik, M. A. G. Laso, T. Lopetegi, and M. Sorolla, "Design method for satellite output multiplexer low-pass filters exhibiting spurious-free frequency behavior and high-power operation," *Microwave Opt. Technol. Lett.*, vol. 52, no. 8, pp. 1724–1728, Aug. 2010.

[47] M. El Sabbagh, K. A. Zaki, H.-W. Yao, and M. Yu, "Full-wave analysis of coupling between combline resonators and its application to combline filters with canonical configurations," *IEEE Trans. Microwave Theory Tech.*, vol. 49, no. 12, pp. 2384–2393, Dec. 2001.

[48] P. Harscher, R. Vahldieck, and S. Amari, "Automated filter tuning using generalized low-pass prototype networks and gradient-based parameter extraction," *IEEE Trans. Microwave Theory Tech.*, vol. 49, no. 12, pp. 2532–2538, Dec. 2001.

[49] M. Morelli, I. Hunter, R. Parry, and V. Postoyalko, "Stop-band improvement of rectangular waveguide filters using different width resonators: selection of resonator widths," in *IEEE MTT-S Int. Microwave Symp. Dig.*, Phoenix, AZ, May 2001, pp. 1623–1626.

[50] H. Y. Hwang and S.-W. Yun, "The design of bandpass filters considering frequency dependence of inverters," *Microwave J.*, vol. 45, no. 9, pp. 154–163, Sep. 2002.

[51] R. Balasubramanian and P. Pramanick, "Computer-aided design of H-plane tapered corrugated waveguide bandpass filters," *Int. J. RF Microw. Comput.-Aided Eng.*, vol. 9, no. 1, pp. 14–21, Jan. 1999.

[52] J.-F. Liang and K. A. Zaki, "CAD of microwave junctions by polynomial curve fitting," in *IEEE MTT-S Int. Microwave Symp. Dig.*, Atlanta, GA, Jun. 1993, pp. 451–454.

[53] Y. Rong, H.-W. Yao, K. A. Zaki, and T. G. Dolan, "Millimeter wave Ka-band H-plane diplexers and multiplexers," *IEEE Trans. Microwave Theory Tech.*, vol. 47, no. 12, pp. 2325–2330, Dec. 1999.

[54] *HFSS Manual*, Ansoft, LLC, Pittsburgh, PA, 2008, release 11.1.3.

[55] R. J. Wenzel, "Exact theory of interdigital bandpass filters and related coupled structures," *IEEE Trans. Microwave Theory Tech.*, vol. 13, no. 9, pp. 559–575, Sep. 1965.

[56] N. A. McDonald, "Electric and magnetic coupling through small apertures in shield walls of any thickness," *IEEE Trans. Microwave Theory Tech.*, vol. 20, no. 10, pp. 689–695, Oct. 1972.

[57] H.-W. Yao, K. A. Zaki, A. E. Atia, and R. Hershtig, "Full wave modeling of conducting posts in rectangular waveguides and its applications to slot coupled combline filters," *IEEE Trans. Microwave Theory Tech.*, vol. 43, no. 12, pp. 2824–2830, Dec. 1995.

[58] A. Morini, G. Venanzoni, M. Farina, and T. Rozzi, "Modified adaptive prototype inclusive of the external couplings for the design of coaxial filters," *IEEE Trans. Microwave Theory Tech.*, vol. 55, no. 9, pp. 1905–1911, Sep. 2007.

[59] A. Atia and A. Williams, "Narrow-bandpass waveguide filters," *IEEE Trans. Microwave Theory Tech.*, vol. 20, no. 4, pp. 258–265, Apr. 1972.

[60] A. Atia, A. Williams, and R. Newcomb, "Narrow-band multiple-coupled cavity synthesis," *IEEE Trans. Circuits Syst.*, vol. 21, no. 5, pp. 649–655, Sep. 1974.

[61] A. Atia and A. Williams, "New types of bandpass filters for satellite transponders," *COMSAT Tech. Rev.*, vol. 1, pp. 21–43, 1971.

[62] J.-F. Liang, X.-P. Liang, K. A. Zaki, and A. E. Atia, "Dual-mode dielectric or air-filled rectangular waveguide filters," *IEEE Trans. Microwave Theory Tech.*, vol. 42, no. 7, pp. 1330–1336, Jul. 1994.

[63] K.-L. Wu, "An optimal circular-waveguide dual-mode filter without tuning screws," *IEEE Trans. Microwave Theory Tech.*, vol. 47, no. 3, pp. 271–276, Mar. 1999.

[64] J. R. Montejo and J. Zapata, "Full-wave design and realization of multicoupled dual-mode circular waveguide filters," *IEEE Trans. Microwave Theory Tech.*, vol. 43, no. 6, pp. 1290–1297, Jun. 1995.

Vicente E. Boria (S'91-A'99-SM'02) was born in Valencia, Spain, on May 18, 1970. He received the "Ingeniero de Telecomunicación" degree (with first-class honors) and the "Doctor Ingeniero de Telecomunicación" degree from the Universidad Politécnica de Valencia, Spain, in 1993 and 1997, respectively.

In 1993 he joined the "Departamento de Comunicaciones", Universidad Politécnica de Valencia, where he is Full Professor since 2003. In 1995 and 1996 he was held a Spanish Trainee position with the European Space Research and Technology Centre (ESTEC)-European Space Agency (ESA), Noordwijk, The Netherlands, where he was involved in the area of EM analysis and design of passive waveguide devices. He has authored or co-authored 7 chapters in technical textbooks, 70 papers in refereed international technical journals and over 150 papers in international conference proceedings. His current research interests include numerical methods for the analysis of waveguide and scattering structures, automated design of waveguide components, radiating systems, measurement techniques, and power effects (multipactor and corona) in waveguide systems.

Dr. Boria is a member of the IEEE Microwave Theory and Techniques Society (IEEE MTT-S) and the IEEE Antennas and Propagation Society (IEEE AP-S) since 1992. He serves on the Editorial Boards of the IEEE Transactions on Microwave Theory and Techniques and IEEE Microwave and Wireless Components Letters. He is also member of the Technical Committees of the IEEE-MTT International Microwave Symposium and of the European Microwave Conference. He was the recipient of the 2001 Social Council of Universidad Politécnica de Valencia First Research Prize for his outstanding activity during 1995-2000.

Pablo Soto (S'01-M'06) was born in 1975 in Cartagena, Spain. He received the M.S. degree in Telecommunication Engineering from the Universidad Politécnica de Valencia in 1999, where he is currently working toward the Ph.D. degree.

In 2000 he joined the Departamento de Comunicaciones, Universidad Politécnica de Valencia, where he is Lecturer since 2002. In 2000 he was a fellow with the European Space Research and Technology Centre (ESTEC-ESA), Noordwijk, the Netherlands. His research interests comprise numerical methods for the analysis, synthesis and automated design of passive waveguide components. Mr. Soto received the 2000 COIT/AEIT national award to the best Master Thesis in Basic Information and Communication Technologies.

Santiago Cogollos was born in Valencia, Spain, on January 15, 1972. He received the degree in telecommunication engineering and the Ph.D. degree from Technical University of Valencia, Valencia, Spain, in 1996 and 2002, respectively. In 2000 he joined the Communications Department of the Technical University of Valencia, where he was an Assistant Lecturer from 2000 to 2001, a Lecturer from 2001 to 2002, and became an Associate Professor in 2002. He has collaborated with the European Space Research and Technology Centre of the European Space Agency in the development of modal analysis tools for payload systems in satellites. In 2005 he held a post doctoral research position working in the area of new synthesis techniques in filter design at University of Waterloo, Waterloo, Ont., Canada. His current research interests include applied electromagnetics, mathematical methods for electromagnetic theory, analytical and numerical methods for the analysis of waveguide structures, and design of waveguide components for space applications.